Cancer Letters 467 (2019) 1–8

Contents lists available at ScienceDirect

Cancer Letters

journal homepage: www.elsevier.com/locate/canlet

Original Articles

Antibiotic treatment ameliorates Ten-eleven translocation 2 (TET2) loss-of-function associated hematological malignancies

Hongxiang Zeng[a,1], Hailan He[a,b,1], Lei Guo[a], Jia Li[a], Minjung Lee[a], Wei Han[a], Anna G. Guzman[c,d], Shengbing Zang[e], Yubin Zhou[f], Xiaotian Zhang[g], Margaret A. Goodell[c,d,h,i], Katherine Y. King[c,d,j], Deqiang Sun[a,**], Yun Huang[a,*]

[a] Center for Epigenetics & Disease Prevention, Institute of Biosciences and Technology, Texas A&M University, Houston, TX, 77030, USA
[b] Department of Colorectal and Anal Surgery, Xinhua Hospital, Shanghai Jiao Tong University School of Medicine, Shanghai, 200092, China
[c] Stem Cells and Regenerative Medicine Center, Baylor College of Medicine, Houston, TX, 77030, USA
[d] Center for Cell and Gene Therapy, Baylor College of Medicine, Houston, TX, 77030, USA
[e] Department of Pathology, Sun Yat-sen University Cancer Center, Guangzhou, 510060, China
[f] Center for Translational Cancer Research, Institute of Biosciences and Technology, Texas A&M University, Houston, TX, 77030, USA
[g] Van Andel Institute, Center for Epigenetics, Grand Rapids, MI, 49503, USA
[h] Program in Developmental Biology, Baylor College of Medicine, Houston, TX, 77030, USA
[i] Department of Molecular and Human Genetics, Baylor College of Medicine, Houston, TX, 77030, USA
[j] Department of Pediatrics, Section of Infectious Diseases, Baylor College of Medicine, Houston, TX, 77030, USA

ARTICLE INFO

Keywords:
Epigenetics
TET2
Hematological malignancies
Inflammation
Antibiotics

ABSTRACT

TET2 is among the most frequently mutated genes in hematological malignancies, as well as in healthy individuals with clonal hematopoiesis. Inflammatory stress is known to promote the expansion of *Tet2*-deficient hematopoietic stem cells, as well as the initiation of pre-leukemic conditions. Infection is one of the most frequent complications in hematological malignancies and antibiotics are commonly used to suppress infection-induced inflammation, but their application in *TET2* mutation-associated cancers remained underexplored. In this study, we discovered that Tet2 depletion led to aberrant expansion of myeloid cells, which was correlated with elevated serum levels of pro-inflammatory cytokines at the pre-malignant stage. Antibiotics treatment suppressed the growth of *Tet2*-deficient myeloid and lymphoid tumor cells *in vivo*. Transcriptomic profiling further revealed significant changes in the expression of genes involved in the TNF-α signaling and other immunomodulatory pathways in antibiotics-treated tumor cells. Pharmacological inhibition of TNF-α signaling partially attenuated *Tet2*-deficient tumor cell growth *in vivo*. Therefore, our findings establish the feasibility of targeting pro-inflammatory pathways to curtail *TET2* inactivation-associated hematological malignancies.

1. Introduction

Ten-eleven Translocation 2 (TET2), a 5-methylcytosine dioxygenase, is frequently mutated in myeloid and lymphoid malignancies [1–4]. *TET2* mutations are found in approximately 60% patients with chronic myelomonocytic leukemia (CMML) [5–7] and in 10–83% of patients with T cell lymphomas [8,9]. However, *TET2* mutations are also detected in healthy individuals with clonal hematopoiesis [10], suggesting that additional factors might be required to promote the malignant transformation of *TET2*-defective blood cells. Although *Tet2*-deficent mice show increased numbers of hematopoietic stem progenitor cells (HSPCs) and myeloid bias during HSPCs lineage specification, they seldom develop hematological malignancies [1,8,11–13]. Other factors, such as additional genetic defects [14–18] and immunostimulation [19,20], are required to promote the full blown tumors. Therefore, these additional factors might serve as alternative therapeutic targets to treat cancers associated with *TET2* mutations.

Deregulation of innate immunity and inflammatory signaling is closely associated with the occurrence of hematological malignancies [21]. Pro-inflammatory signals, arising from the tumor necrosis factor-α (TNF-α), Toll-like receptors (TLRs) and/or interferon (IFN) pathways, can alter the proliferation, differentiation and self-renewal of HSPCs

* Corresponding author.
** Corresponding author.
E-mail addresses: dsun@tamu.edu (D. Sun), yun.huang@tamu.edu (Y. Huang).
[1] These authors contributed equally to the work.

https://doi.org/10.1016/j.canlet.2019.09.013
Received 23 August 2019; Received in revised form 22 September 2019; Accepted 24 September 2019
0304-3835/ © 2019 Elsevier B.V. All rights reserved.

[22,23]. Under pathophysiological conditions, epidemiological studies have revealed a strong positive correlation between autoimmune disorders and the incidence of myelodysplastic syndromes (MDS) [24]. Autoimmune phenotypes are also frequently observed in patients with T cell lymphomas [25]. Under inflammatory stress induced by lipopolysaccharides (LPS) or abnormal interleukin-6 (IL-6) production by microbiota [19,20], *Tet2* deficient murine HSPCs exhibit a growth advantage, suggesting that inflammatory signaling could promote the malignant transformation of *Tet2*-deficient preleukemic HSPCs. Conversely, *TET2*-depleted malignant cells per se tend to enhance immune response and induce inflammation in the host.

Infection is one of the most frequent complications in patients with hematological malignancies, such as CMML and lymphoma [26]. Antibiotics are commonly used in cancer patients to fight against pathogen invasion and to attenuate the inflammatory response under pathological conditions. However prolonged treatment with antibiotics tends to disrupt the gut microbiota homeostasis and impair normal hematopoiesis [27,28]. The therapeutic potential of antibiotics in the treatment of *TET2*-defective malignancies remains largely underexplored. In this study, we use CMML-like or $CD4^+$ lymphoma derived from *Tet2*-deficient mice as the model systems to investigate whether and how antibiotic treatment impinges on tumor progression *in vivo*.

2. Materials and methods

2.1. Animal models and adoptive cell transfer

Animal studies were approved by the Institutional Animal Care Use Committee (IACUC) of the Institute of Biosciences and Technology, Texas A&M University. The Tet2KO mouse strain was reported previously [12]. CD45.1 recipient mice (B6.SJL-Ptprca Pepcb/BoyJ) were purchased from the Jackson Laboratory (Stock No: 002014). CMML-like (Gr1 + Mac1 +) cells were enriched in the bone marrow of Tet2KO mice and $CD4^+$ lymphoma ($CD4^+$) cells were purified from the spleen of Tet2KO mice. 2×10^6 cells were resuspended in 200 μl PBS and retro-orbitally injected into sub-lethally irradiated CD45.1 recipient mice (6–8 weeks old, female). The reconstitution efficiency of tumor cells was assessed by examining the CD45.2 + cells from peripheral blood in the recipient mice 3 weeks after adoptive cell transfer.

2.2. Antibiotics and inhibitors

Mice were fed with water for 10 days with an antibiotics cocktail containing the following: 1 g/L ampicillin (cat#: 45000–612), 0.5 g/L vancomycin (cat#: 97062–554), 1 g/L neomycin (cat#: 97061–908) and 1 g/L metronidazole (cat#: BT134695; VWR) as previously reported [27]. Flavoring (20 g/L grape flavored Kool-Aid Drink) was added in the drinking water for all groups. The TNF-α inhibitor CC4047 (also called pomalidomide; Cat#:S1567) was purchased from Selleckchem and dissolved in 2% DMSO + 30% PEG 300 + 2% Tween 80 + ddH_2O. The inhibitor was administered by intraperitoneal injection at a dose of 7 mg/kg mice every day for 10 consecutive days.

2.3. Histological analysis

All collected tissues were fixed in 10% neutral-buffered formalin for 24 h at 4 °C. The tissue blocks were embedded in the paraffin after specimens treated with gradient alcohol dehydration. 7 μm-thick slices were cut for Hematoxylin and Eosin (H&E) staining. IHC staining was performed using the ImmPRESSTIM polymer detection system (Vector Laboratories) according to the manufacturer's instructions. Anti-CD3 (Abcam ab16669, 1:150) was used. All the slides were analyzed under a Nikon upright microscope.

2.4. Flow cytometry analysis

Bone marrow was harvested by flushing two femurs and two tibias. Cells were re-suspended in FACS buffer (PBS with 0.1% BSA, 2 mM EDTA) and incubated with anti-CD16/32 (ThermoFisher Scientific 14-0161-82, 1:200) for 15 min on ice. Cells were then incubated with indicated antibodies for 30 min at 4 °C in the dark, followed by washing with FACS buffer twice. For mouse lineage analysis in spleen and bone marrow, Mac-1 (ThermoFisher Scientific M1/70, 1:200) and Gr-1 (ThermoFisher Scientific RB6-8C5, 1:200) cells were used to define the myeloid lineage; CD4 (ThermoFisher Scientific GK1.5, 1:200) and CD8 (ThermoFisher Scientific 5H10-1, 1:200) were used to define the T cell lineage; B220 (ThermoFisher Scientific RA3-6B2, 1:200) and CD19 (ThermoFisher Scientific eBio1D3, 1:200) were used to define the B cell lineage; Ter119 (BioLegend Ter119, 1:100) and CD71 (BioLegend RI7217, 1:50) were used to define the erythroid lineage. For the bone marrow hematopoietic progenitor stem cell (HSPCs) analysis, a panel of biotin-conjugated antibodies against Ter-119 (BioLegend Ter119, 1:50), Gr1 (BioLegend RB6-8C5, 1:50), Mac-1 (BioLegend M1/70, 1:50), B220 (BioLegend RA3-6B2, 1:50), CD3 (BioLegend 17A2, 1:50) surface antigens were mixed as a cocktail for lineage labeling. A panel of antibodies containing Lin-biotin cocktail, Streptavidin-eFluor®450 (ThermoFisher Scientific 48-4317-82, 1:400), c-Kit APC (ThermoFisher Scientific 2B8, 1:200), Sca-1 PE/Cy7 (ThermoFisher Scientific D7, 1:200), CD150 PE (BioLegend TC15-12F12.2, 1:100) and CD48 FITC (BioLegend HM48-1, 1:100) were used for LSK/HSC labeling. A panel of antibodies containing Lin-biotin cocktail plus biotin-conjugated CD127 (ThermoFisher Scientific A7R34, 1:50), streptavidin-eFluor®450 (ThermoFisher Scientific 48-4317-82, 1:400), c-Kit APC (ThermoFisher Scientific 2B8, 1:200), Sca-1PE/Cy7 (ThermoFisher Scientific D7, 1:200), CD16/32-PE (ThermoFisher Scientific 93, 1:200) and CD34 FITC (ThermoFisher Scientific RAM34, 1:200) were used for CMP/GMP/MEP labeling. Flow cytometry analysis was performed using LSRII (BD Biosciences) and data were analyzed with the FlowJo10 software package (FlowJo,LLC).

2.5. ELISA

Blood cells were collected by retro-orbital sinus puncture into 1.5 ml eppendorf tubes. Blood was allowed to clot at room temperature for 60 min before spinning at 3000 rpm for 15 min at 4 °C. IFN gamma was measured by mouse IFN gamma ELISA Ready-set-go kit (ebioscience™, 88–7314), IL-1 beta was measured by eBioscience™ Mouse IL-1 beta ELISA Ready-SET-Go Kit (eBioscience™, 501129749), TNF alpha was measured by eBioscience™ Mouse TNF alpha ELISA Ready-SET-Go Kit (ebioscience™, 50-112-8954), IL-6 was measured by eBioscience™ Mouse IL-6 beta ELISA Ready-SET-Go Kit (ebioscience™, 50-172-18). The signal was detected using BioTek Cytation 5 Instrument at 450 nm (Fisher Scientific).

2.6. Real-time quantitative PCR (qPCR)

Total RNA was isolated from the RNeasy mini kit (Qiagen) according to the manufacturer's instructions, followed by reverse transcription using an AmfiRivert Platinum One cDNA Synthesis Master Mix (GenDEPOT). Real-time PCR (RT-PCR) was performed by using amfiSure qGreen Q-PCR Master Mix reagents (GenDEPOT) and LightCycler 96 real-time PCR system (Roche). Data were analyzed using the LightCycler software. The gene expression level was normalized to Gapdh. Primer sequences used for real-time RT-PCR were listed below:

Nfkbia forward: TGCCTGGCCAGTGTAGCAGTCTT
Nfkbia reverse: CAAAGTCACCAAGTGCTCCACGAT
Sgk1 forward: TCCTGAGGATGGGACATTTTCA
Sgk1 reverse: CTGCTCGAAGCACCCTTACC
Traf1 forward: CACTCCAGTTCTGTTTCCT

Traf1 reverse: CATATCCACTCTCTCTTCTCAC
Tnfaip2 forward: AGGAGGAGTCTGCGAAGAAGA
Tnfaip2 reverse: GGCAGTGGACCATCTAACTCG
B4galt1 forward: CACCACCACTGGACTGTTGT
B4galt1 reverse: ATGGGATGATGATGGCCACC
Nfil3 forward: TTCCCCCTCACGGACCAGGGA
Nfil3 forward: CATGGCGTCTTTCTTCTCGTCCGG
Gapdh forward: TCAACAGCAACTCCCACTCTTCCA
Gapdh reverse: ACCCTGTTGCTGTAGCCGTATTCA

2.7. Western blotting

Cells were lysed with TNTE buffer (150 mM NaCl, 50 mM Tris-HCl, pH 7.5, 0.5% Triton X-100, 5 mM EDTA) supplemented with a protease inhibitor cocktail (GenDEPOT) and phosphatase inhibitor tablet (Sigma), and incubated on ice for 15 min. Cell debris was removed by centrifuging at 13,000 rpm for 10 min at 4 °C. The protein was quantified by a Pierce BCA protein assay kit (Thermo Fisher Scientific). Samples were mixed with SDS sample buffer at 95 °C for 15 min. Proteins were detected by using the West-Q Pico Dura ECL kit (GenDEPOT). Primary antibodies used for immunoblotting: Anti-Gapdh (Sigma G9545, 1:3000), Anti-Phospho–NF–κB p65 (Ser536) (Cell Signaling Technology 93H1 cat# 3033, 1:1000) Rabbit mAb, and Anti-NF-κB p65 (Cell Signaling Technology D14E12, cat# 8242, 1:1000) XP® Rabbit mAb.

2.8. Feces collection and bacterial culture

Fresh feces (2–3 pellets/mice) were collected from individual mice in an autoclaved chamber and dissolved in 1.5 ml PBS. The mixture were left on the bench for 20–30 min to allow debris to settle. Then the supernatant (50 μl) was gently transferred from each fecal homogenate onto a LB agar plate and incubated at 37 °C overnight.

2.9. RNA-seq library construction and data analysis

Total RNA was extracted from cells (n = 2 per condition) using the RNeasy mini kit (Qiagen) following manufacturer's instructions. Poly A tail enriched RNA was enriched using a Poly(A)Purist Kit (Thermo Fisher Scientific), followed by RNA-seq library preparation using an Ultra directional RNA library prep kit for Illumina (NEB) per manufacturer's instruction. RNA-seq was performed using the Illumina Nextseq500 with the 75 bp single-ended running mode. The reads were mapped to mm10 using Bowtie2 with default parameters. The RefSeq gene annotation was obtained from the UCSC genome database. The number of reads mapped to each gene was counted using HTSeq (-m intersection-nonempty, -s no, -t exon, -i gene_id, http://www.huber.embl.de/users/anders/HTSeq/) with uniquely mapped reads as input. RPKM values were calculated with the raw read counts across all genes. The differentially expressed genes among the experimental groups were identified with negative binomial tests for pairwise comparisons between corresponding groups by employing the Bioconductor package DESeq2 using a corrected p value ≤ 0.05 and fold change thresholds of ≥ 2 or ≤ 0.5. GSEA function were used to analyze the function of significantly differentially expressed genes between two conditions. The Pearson correlation were used to compare reproducibility of all the analyzed samples. For the heat maps, row-wise scaled RPKM values across all samples were plotted using the function heatmap.2 in the R package gplots (www.r-project.org).

2.10. Accession numbers

The RNA-seq datasets have been deposited into GEO under the accession number GSE129886.

3. Results

3.1. Tet2 deficiency leads to variegated outcomes in the murine hematological system

Upon genetic ablation of *Tet2*, we observed spontaneous occurrence of hematological malignancies in Tet2 knockout (Tet2KO) mice, which exhibited a median survival of ~340 days (red curve, Fig. S1A). By comparison, no gross abnormalities were observed in wild-type (WT) mice with the same genetic background during the 600-day experimental window. As revealed by histopathological and flow cytometry analyses, Tet2KO mice (n = 40) developed a wide spectrum of hematological malignancies, including myeloid (73%), T cell (23%), and B cell (4%) malignancies (Fig. S1B). We further carried out histological analyses on major organs collected from Tet2KO mice before disease onset (disease free, DF), and Tet2KO mice which had developed T cell lymphoma or CMML (Fig. S1C). In Tet2KO mice with lymphoma, we observed disruption of the lymph node structure as well as $CD3^+$ tumor cell infiltration in the liver (Fig. S1C, middle panel). In Tet2KO mice with CMML, we observed significantly increased numbers of monocytes and immature blood cells in the peripheral blood (Fig. S1C, right panel). To further characterize the malignant phenotypes, we performed flow cytometric analysis to identify the affected cell types in Tet2KO mice (Figs. S1D–F). In Tet2KO mice with CMML, we observed a significant expansion of Gr1 + Mac1 + myeloid cells in both bone marrow and spleen, along with notable extramedullary hematopoiesis marked by an increase of CD71 + Ter119 + erythroid cells in peripheral lymphoid tissues (Figs. S1E–F). In Tet2KO mice with lymphoma, we observed a pronounced augmentation of $CD4^+$ T cells in both bone marrow and spleen. No appreciable pathological phenotypes were found in Tet2KO mice before disease onset (< 6-months-old; Fig. S1C, Figs. S2A–C). Clearly, genetic depletion of Tet2 in mice led to the development of various hematological malignancies, a finding that concurs with recent observations reported by other groups [29].

3.2. Positive correlation between serum cytokine levels and myeloid expansion in Tet2KO mice

Bacterial translocation-induced IL-6 production has been recently shown to promote the expansion of Tet2KO myeloid cells and drive preleukemic myeloproliferation [19]. To examine the correlation between cytokine production and myeloid expansion in Tet2KO mice, we measured the level of key pro-inflammatory cytokines, including IL-1, TNF-α, IL-6 and IFN-γ, in the serum of age- (16 weeks old) and gender-matched WT and Tet2KO mice before tumor onset. We observed significant upregulation of IL-1 and TNF-α levels in Tet2KO mice compared with the WT group (Fig. 1A). Next, we measured the percentage of Gr1 + Mac1 + myeloid cells in the peripheral blood obtained from both WT and Tet2KO mice, with the goal of establishing the correlation between serum cytokine levels and myeloid cell expansion. We observed a strong positive correlation between the IL1 or TNF-α levels and the percentage of myeloid cells in the peripheral blood for the Tet2KO group but not the WT group (Fig. 1B). These data are consistent with the previously reported correlation between chronic inflammatory conditions and myeloid malignancies [30].

In order to identify the pathways that are important to promote the malignant transformation of *Tet2*-deficient blood cells, we next compared the transcriptome profiles of *Tet2*-deficient non-cancerous (Tet2KO lin^-cKit^+ (LK) or $CD4^+$ T cells, isolated from mice < 6 months old and disease free) and tumor tissues (Tet2KO $lin^-cKit^+Mac1^+Gr1^+$ CMML-like or $CD4^+$ lymphoma cells) using RNA-seq (Fig. S3A). We identified a total of 8,501 differentially expressed genes (DEGs) between Tet2KO LK cells and Tet2KO CMML-like cells, and 4,755 DEGs between Tet2KO $CD4^+$ T cells and Tet2KO lymphoma cells (Fig. 1C). In order to identify the common affected genes by Tet2 deletion, we identified total of 2,754 overlapped DEGs between tumor-

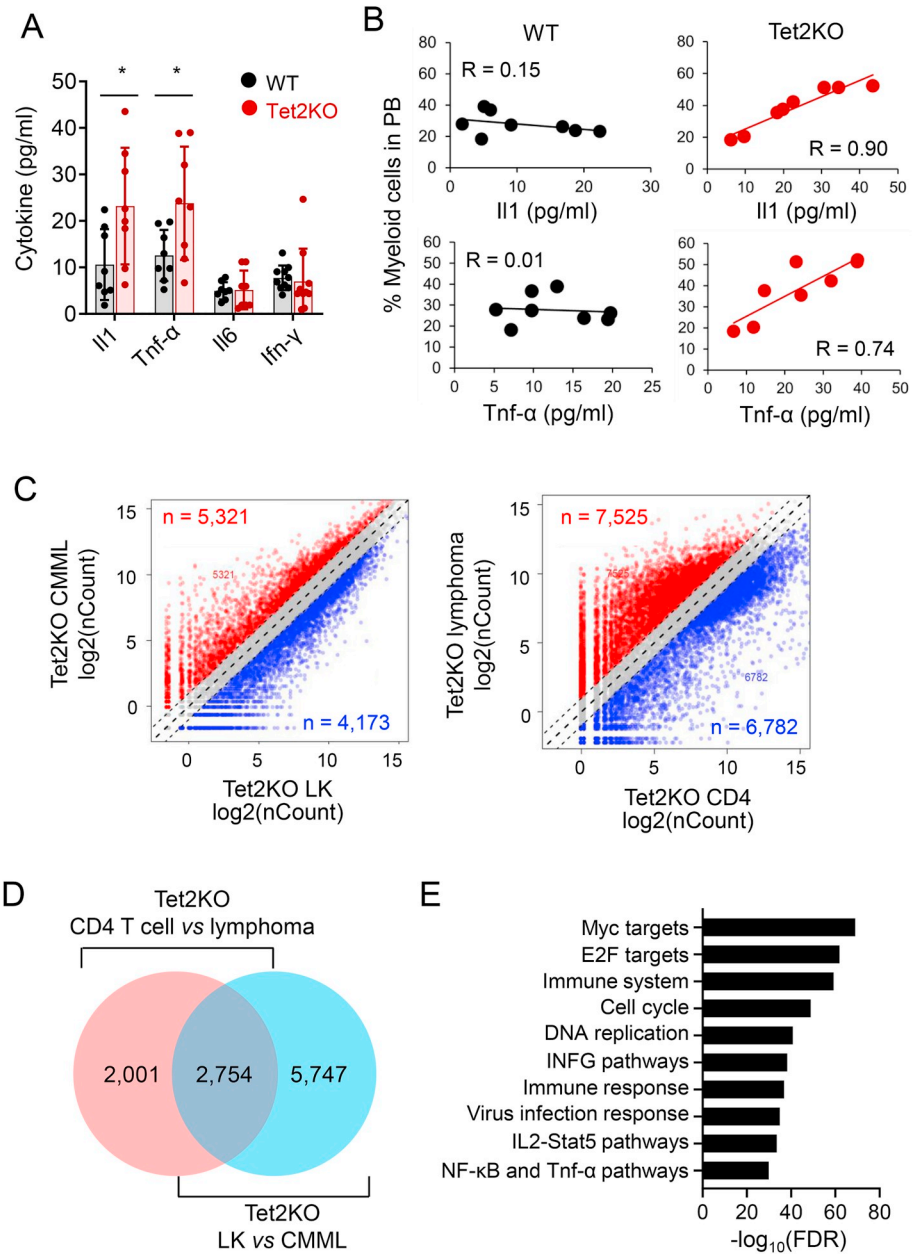

Fig. 1. Tet2KO malignant cells displayed an abnormal innate immune phenotype.
(A) Serum cytokine levels (IL-1, TNF-α, IL-6 and IFN-γ) measured in the peripheral blood of WT and Tet2KO mice. (n = 8 mice per group, *p < 0.05, by two-tailed Student's *t*-test)
(B) The correlation between the percentage of myeloid cells (Mac1 + Gr1 +) and serum cytokine levels (IL-1 and TNF-α) in WT and Tet2KO mice.
(C) Scatter plot of the RNA-seq expression data to identify differentially expressed genes (DEGs) in Tet2KO LK vs CMML ($Mac1^{+}Gr1^{+}cKit^{high}$) cells (left), and Tet2KO $CD4^{+}$ T cells vs $CD4^{+}$ lymphoma cells (right).
(D) Comparison of differentially expressed genes (DEGs) between $CD4^{+}$ T cells from disease-free Tet2KO mice and Tet2KO $CD4^{+}$ lymphoma cells, or between Lin-Kit + cells from disease-free Tet2KO mice and Tet2KO CMML-like cells.
(E) GSEA analysis of overlapping DEGs (n = 3,039) depicted in panel (C).

free and malignant cells (Fig. 1D). Further Gene Set Enrichment Analysis (GSEA) showed that the top identified DEGs included Myc and E2F target genes, as well as genes associated with key immunoinflammatory signaling pathways (Fig. 1E), including the TNF pathways. Together, both phenotypic and transcriptomic analysis results converged to implicate inflammatory signaling as a key culprit responsible for the pathogenesis of Tet2 inactivation-associated hematological malignancies.

3.3. Antibiotic treatment suppresses the growth of Tet2 deficient hematological malignant cells

Tet2-deficient mice have been reported to exhibit bacterial translocation and aberrant inflammatory responses due to impaired small intestinal barrier function [19]. We reasoned that antibiotics might suppress translocated bacteria-induced immune response, and therefore hold promise to ameliorate infection in patients with hematological malignancies. To test this idea *in vivo*, we adoptively transferred Tet2KO $CD4^{+}$ T cell lymphoma or $Mac1^{+}Gr1^{+}$ CMML-like tumor cells into sub-lethally irradiated CD45.1 recipient mice, followed by the treatment of a four-antibiotic cocktail (ABX treatment) of vancomycin, neomycin, ampicillin, and metronidazole (VNAM) in the drinking water (Fig. 2A). After 10 day ABX treatment, we switched back to normal drinking water without the antibiotics cocktail and monitored the survival of each group (Fig. 2A). Mice transferred with the same type of tumor cells without ABX treatment were used as control. To confirm the effectiveness of antibiotic treatment, we collected the feces of the mice with and without ABX treatment and performed aerobic culture of the supernatant collected from feces. No bacterial were observed in mice treated with the antibiotic cocktail (Fig. S4A). Most notably, antibiotic treatment prolonged the survival of recipient mice (Fig. 2B). By contrast, recipient mice transferred with WT cells showed no difference before and after ABX treatment (Fig. 2B). Upon ABX treatment, we also observed a significant reduction of the spleen size of recipient mice transferred with Tet2KO CMML-like cells (Fig. 2C), which is consistent with previous publication in ABX treated WT mice [27]. To further confirm that antibiotic treatment suppressed Tet2-deficient CMML-like or lymphoma cell growth, we analyzed the percentage of CD45.2 + tumor cells in the peripheral blood of recipient mice 10 days

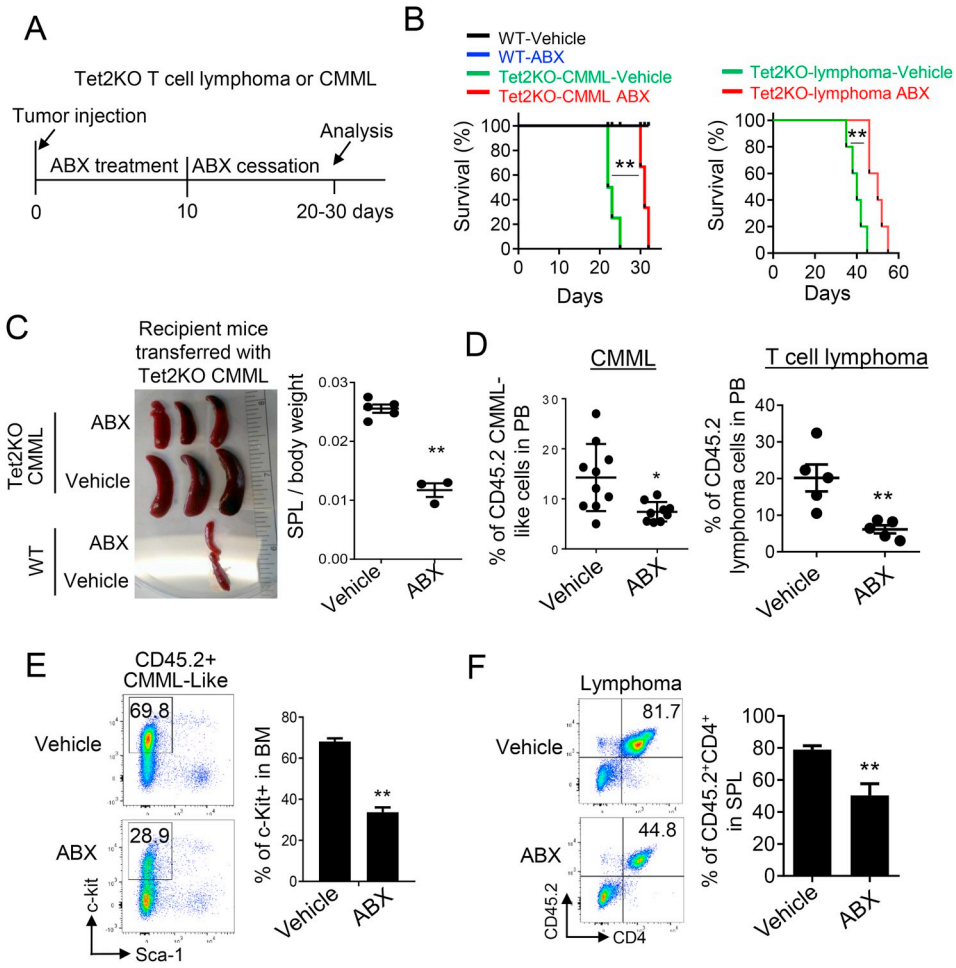

Fig. 2. Antibiotics cocktail (ABX) treatment suppresses the growth of Tet2KO tumor cells in vivo.

(A) Schematic of the experimental design and the timeline of antibiotics (ABX) treatment in CD45.1 recipient mice transferred with Tet2KO CMML or CD4$^+$ lymphoma cells.

(B) (left) Kaplan-Meier survival curves of CD45.1 recipient mice transferred with WT (Mac1 + Gr1 + myeloid cells) and Tet2KO CMML-like tumor cells treated with or without the VNAM antibiotics cocktail (ABX, n = 4 mice in the CMML group; n = 5 mice in the lymphoma group). (right) Kaplan-Meier survival curves of CD45.1 recipient mice transferred with Tet2KO CD4$^+$ lymphoma cells treated with or without the VNAM antibiotics (ABX) cocktail (n = 4 mice). (**p < 0.001, long-rank test).

(C) Representative images of spleens (left) and statistical analysis (right) on the ratio of spleens/total body weight in recipient mice transferred with WT (Mac1 + Gr1 + myeloid cells) or Tet2KO CMML-like tumor cells 26 days after cell injection.

(D) (left) The percentage of CD45.2 + Tet2KO CMML-like cells ((CD45.2$^+$Lin$^-$cfKit$^+$Sca1$^+$)) in the peripheral blood of CD45.1 + recipient mice treated with and without the VNAM antibiotics cocktail for 21 days after cell injection (n = 10 mice per group, *p < 0.05, by two-tailed Student's *t*-test). (right) The percentage of CD45.2$^+$CD4$^+$ Tet2KO lymphoma cells in the spleen of CD45.1 recipient mice treated with and without the VNAM antibiotics cocktail at 36 days after lymphoma cell injection. (n = 5 mice per group, **p < 0.005, two-tailed Student's *t*-test).

(E) Representative flow cytometry (left) and statistical analysis results (right) of CD45.2 + c-Kit + Sca-1 + Tet2KO CMML-like cells in the bone marrow of CD45.1 recipient mice treated with and without the VNAM antibiotics cocktail at 26 days after cell injection. (n = 3 mice per group, **p < 0.005, by 2-tailed student's *t*-test).

(F) Representative flow cytometry (left) and statistical analysis results (right) of CD45.2 + CD4$^+$ Tet2KO T cell lymphoma cells in the spleen of CD45.1 recipient mice treated with and without the VNAM antibiotics cocktail at 36 days after cell injection. (n = 3 mice per group, **p < 0.005, by 2-tailed student's *t*-test).

after antibiotic withdrawal. We observed a strong reduction of CD45.2 + CMML-like or lymphoma cells in the antibiotic treatment group, when compared with the untreated group (Fig. 2D). In parallel, we observed a strong reduction of CD45.2$^+$lin$^-$c-Kit$^+$Sca1$^-$ CMML-like cells or CD45.2 + CD4$^+$ lymphoma cells isolated from the bone marrow or spleen of recipient mice treated with ABX (Fig. 2E–F). As control, no significant difference of Lin- HSPCs and downstream lineages in the bone marrow was observed in recipient mice transferred with WT bone marrow cells, in the presence or absence of ABX treatment 10 days after antibiotics withdrawal (Fig. 3A–B, Fig. S4B). This finding implies that the suppressive effect from antibiotic treatment is specific to Tet2KO malignant cells. In parallel, we monitored the effect of antibiotic treatment on the AF9 murine AML cell line transduced with a retrovirus encoding *MLL-AF9* into lin-cKit + murine bone marrow cells. No suppressive effect was observed in recipient mice transferred with AF9 murine AML cells upon ABX treatment (Fig. 3C). To further investigate whether the antibiotic treatment directly suppresses *Tet2*-deficient malignant cells, we cultured Tet2KO CMML-like cells in methylcellulose with and without ABX treatment. We did not observe a significant difference in the total cell numbers between the ABX treated and untreated groups (Fig. 3D). These results suggest that the observed suppressive effect is not due to direct toxicity imposed by the antibiotics per se.

Antibiotics treatment has been shown to suppress normal hematopoiesis in mice [27]. We therefore examined how ABX treatment impinged on hematopoiesis in disease-free Tet2KO mice. A similar suppressive effect of antibiotics treatment was noted in both the WT and Tet2KO groups (Fig. 3E). Consistent with earlier studies, antibiotics treatment reduced the total cell number in the bone marrow isolated from either WT or Tet2KO mice (Fig. 3E). We also observed a reduction in the cell number of hematopoietic progenitors, including LSK (Lin$^-$Sca1$^+$cKit$^+$), and myeloid progenitors (Figs. S4C–D) in both WT and *Tet2* deficient mice treated with antibiotics cocktail. These findings indicate that *Tet2*-deficient hematopoietic cells in disease-free mice behave that same as normal hematopoietic cells upon treatment with the antibiotics cocktail.

3.4. Antibiotic treatment suppresses TNF-α signaling in Tet2-deficient hematological malignancies

To identify the signaling pathways that contribute to ABX-induced tumor suppressive effect, we performed unbiased transcriptome analysis on *Tet2*-deficient CMML-like and lymphoma cells isolated from recipient mice treated with or without ABX. From the RNA-seq datasets, over 1,000 DEGs were identified from between the antibiotic treated and untreated groups (Fig. 4A, Fig. S5A). A comparison of DEGs between the CMML vs WT and lymphoma vs WT groups further revealed 485 overlapping genes that were altered after ABX treatment in both

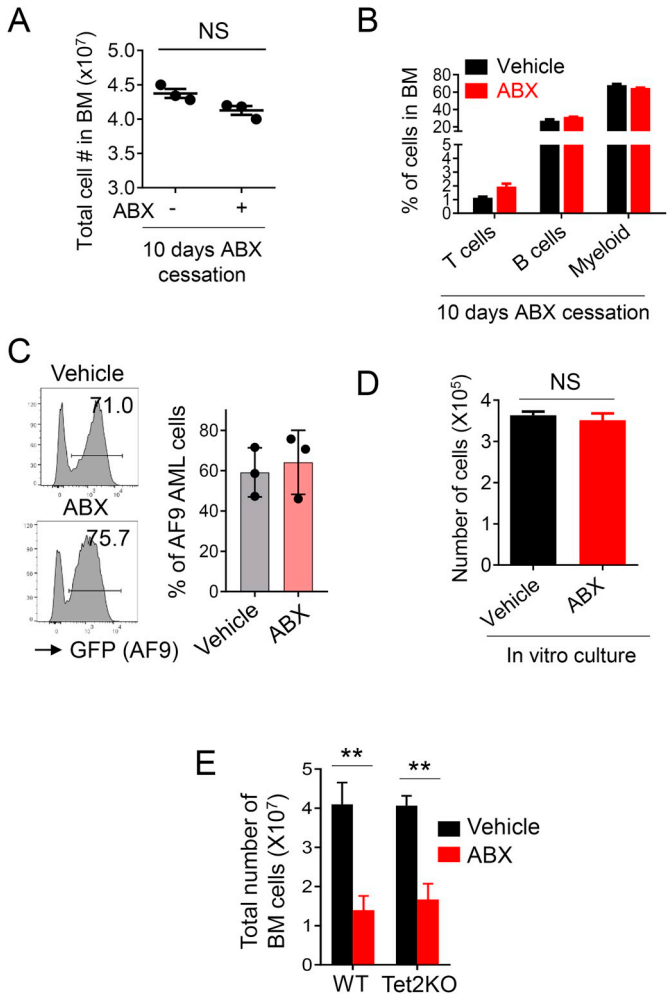

Fig. 3. ABX treatment has no effects on normal hematopoiesis and AML cells bearing WT *Tet2 in vivo* after treatment withdrawal.

(A) The numbers of total bone marrow cells measured in CD45.1 recipient mice treated with and without the VNAM antibiotics cocktail at 26 days after CMML-like cell injection. (n = 3 mice per group)

(B) The percentage of T cells ($CD4^+$ and $CD8^+$), B220 + CD19 + B cells and Gr1 + Mac1 + myeloid cells in bone marrow cells measured in CD45.1 recipient mice treated with and without antibiotics at 26 days after Tet2KO CMML-like cell injection. (n = 3 mice per group)

(C) Flow cytometry profiles (left) and representative statistical analysis (right) of GFP + AF9 AML cells measured in the bone marrow of CD45.1 recipient mice treated with and without the VNAM antibiotics cocktail at 20 days after AML cell injection. (n = 5 mice per group).

(D) Quantification of the numbers of Tet2KO CMML-like cells with and without the VNAM antibiotics cocktail treatment (25 mcg/ml ampicillin, neomycin and metronidazole, 12.5 mcg/ml vancomycin) for 7 days (n = 3 experiments per group). CMML-like cells were cultured *in vitro* with the MethoCult medium.

(E) Statistical analysis of the numbers of total bone marrow cells in normal WT and Tet2KO mice treated the VNAM antibiotics cocktail for 10 days. (n = 3 mice per group, $^{**}p < 0.005$, by 2-tailed student's *t*-test).

cancer types (Fig. 4B, Table S1). GSEA further unveiled that these overlapping genes were closely associated immunomodulation processes, especially those involving the IL2-STAT5 and TNF-α pathways (Fig. 4C–D, Fig. S5B). These data are well aligned with the serum cytokine ELISA analysis results, in which upregulation of TNF-α was positively correlated with myeloid cell expansion in Tet2KO mice (Fig. 1B). With real-time quantitative PCR, we further confirmed dysregulation of key genes involved in TNF-α signaling pathways in tumor cells isolated from the recipient mice after ABX treatment (Fig. 4E).

To further confirm that TNF-α signaling pathway is a major target during antibiotic treatment *in vivo*, we treated recipient mice transferred with Tet2KO CMML-like or lymphoma tumor cells with a TNF-α inhibitor, CC4047 (Fig. 4F). We observed a partial suppression of tumor growth in recipient mice treated with CC4047 for 10 days (Fig. 4G–H). Immunoblot analysis further confirmed the decrease of the phosphorylated NF-κB p65 level, a downstream target of TNF-α in the CC4047 treated group (Fig. S5C), thereby suggesting an efficient suppression of the TNF-α signaling pathway. These data demonstrated that the growth of Tet2-deficient hematological malignant cells partially depend on TNF-α signaling, and that antibiotic treatment suppresses tumor growth by altering TNF-α signaling.

4. Discussion

In the current study, we observed the development of different types of hematological malignancies in aged Tet2KO mice. Clearly, *Tet2* deficiency increases the risk of malignant transformation in the hematopoietic system. Although it is still unclear how *Tet2*-deficient HSPCs are transformed to malignant cells, several studies have documented that *Tet2*-deficient HSPCs exhibit a growth advantage when responding to inflammatory stress [20] and that the incidence of *Tet2/3* deficient T cell lymphoma requires TCR signaling [31]. In the current study, we further observed a strong positive correlation between myeloid expansion and the serum pro-inflammatory cytokine levels in Tet2KO mice, but not in WT mice, suggesting that the inflammatory signaling might stimulate the expansion of Tet2KO HSPCs and ultimately lead to uncontrolled proliferation of *Tet2*-deficient cells.

To seek potential molecular mechanisms, we subsequently the gene expression profiles in two types of *Tet2*-deficient malignant tumor cells (CMML-like and T cell lymphoma cells) by using LK and $CD4^+$ T cells as controls, respectively. We found genes involved in inflammation and cytokine signaling pathways are significantly altered in malignant cells. It still remains unclear how serum pro-inflammatory factors (Il-1 and TNF-α) are upregulated in Tet2-deficient mice. Previous studies reported that *Tet2* depletion in mice tends to disrupt the intestinal barrier to cause aberrant bacterial translocation and cytokine production [19]. We therefore performed antibiotics treatment to reduce infection-mediated inflammatory response in recipient mice transferred with Tet2KO tumor cells. We observed that antibiotics treatment could suppress normal hematopoiesis in both WT and Tet2KO mice during the treatment. 10 days after antibiotics cessation, WT HSPCs could recover from hematopoiesis, which is consistent with an earlier report [27]. By comparison, the suppressive effect remained persistent in Tet2-deficient hematological malignant cells even after antibiotics withdrawal. Additionally, antibiotics treatment alone has no effect on *MLL-AF9* AML cells, suggesting that antibiotics-mediated suppressive effect is specific to Tet2 deficient leukemia and lymphoma cells. This observation is consistent with previous report that inflammatory factors, such as TNF-α, favor *Tet2*-deficient clonal hematopoiesis [30]. Mechanistically, results from our RNA-seq and pharmacological inhibition studies point to the TNF-α signaling pathway as an important target to suppress tumor growth. At the current stage, it still remains unsolved how TNF-α signaling is activated and how antibiotic treatment suppresses TNF-related pathways in *TET2*-mutant malignancies *in vivo*. Based on a previous study [32], hematological neoplasms-associated mutations within TET2 might alter its catalytic activity and result in impaired DNA methylation and hydroxymethylation in the genome. The dysregulation of the TNF-α signaling observed in Tet2-deficient malignant cells might partially arise from abnormal DNA methylation and/or hydroxymethylation. Regardless, our findings establish that suppressing inflammatory pathways with antibiotics might benefit the clinical management of patients bearing hematological malignancies with somatic *TET2* mutations.

Author contributions

YH directed and oversaw the project. HZ, HH and LG performed the

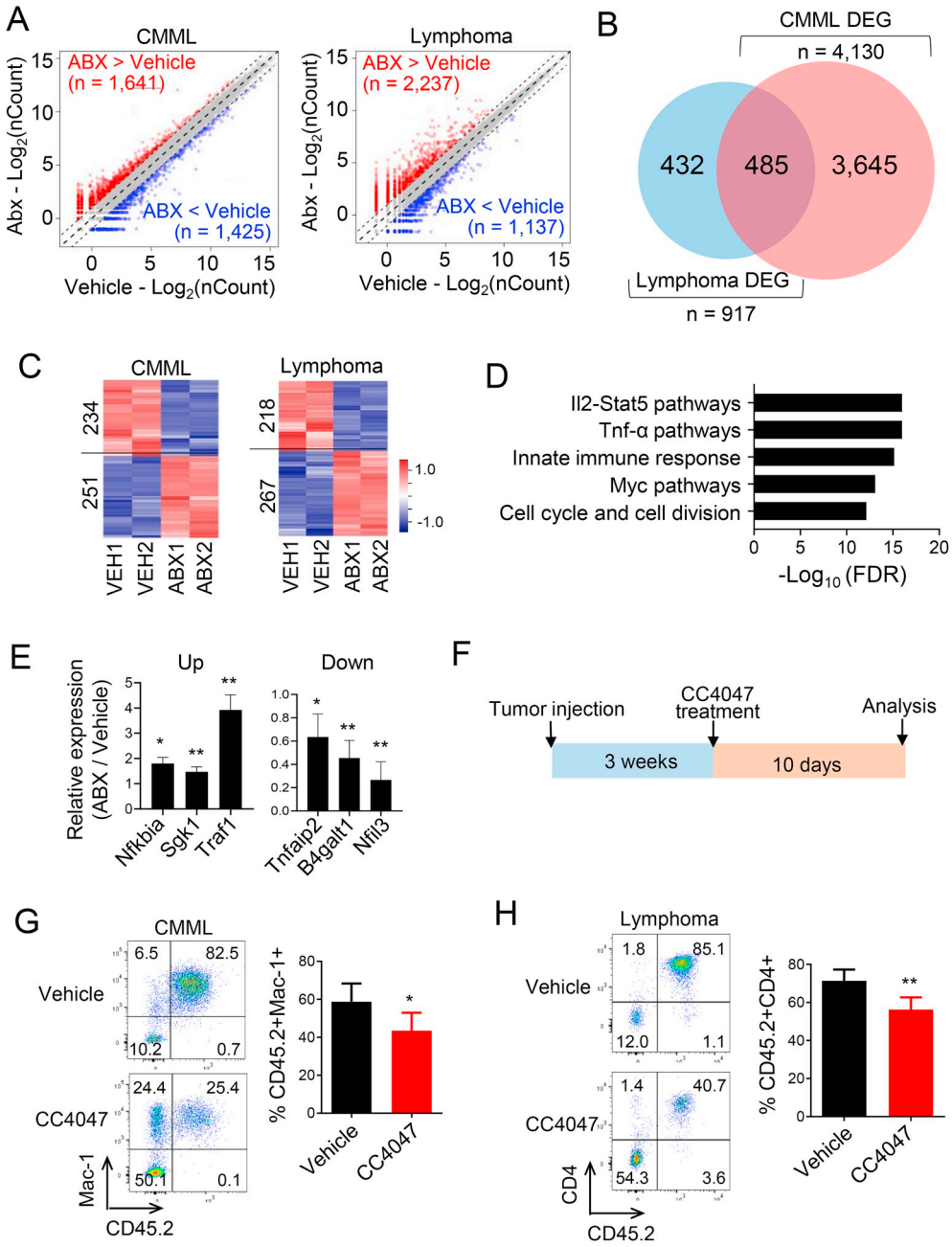

Fig. 4. Antibiotics treatment suppresses immune related signaling pathways in Tet2KO malignant cells.

(A) Scatter plot of the RNA-seq expression data to identify differentially expressed genes (DEGs) in Tet2KO CMML-like cells (left) and Tet2KO CD4$^+$ lymphoma cells (right) between the vehicle and the antibiotics cocktail treatment (ABX) groups.

(B) Venn diagram showing the overlapping DEGs identified from the Tet2KO CMML-like and lymphoma groups treated with and without the VNAM antibiotics cocktail.

(C) Heatmap representation of DGEs identified in Tet2KO CMML (left) or CD4$^+$ lymphomas treated with and without the VNAM antibiotics cocktail.

(D) GSEA analysis of overlapping DEGs identified in both the Tet2KO CMML and CD4$^+$ lymphoma groups treated with and without the VNAM antibiotics cocktail.

(E) Use of qPCR to determine the relative expression of selected DEGs involved in the TNF-α pathway (ABX-over-vehicle ratio). (n = 3, *$p < 0.05$, **$p < 0.005$, by two-tailed Student's *t*-test).

(F) Experimental design of recipient mice transferred with Tet2KO CMML-like or CD4$^+$ lymphoma cells treated with TNF-α inhibitor, CC4074 (also named as Pomalidomide), (7 mg/kg mice every day for 10 days) *in vivo*.

(G) Representative flow cytometry (left) and statistical analysis (right) of CD45.2 + Tet2KO CMML-like cells measured in the peripheral blood of CD45.1 recipient mice treated with and without CC4074 at 30 days after tumor cell injection. (n = 4 mice per group, *$p < 0.05$, by two-tailed Student's *t*-test).

(H) Representative flow cytometry (left) and statistical analysis (right) of CD45.2 + Tet2KO lymphoma cells measured in the peripheral blood of CD45.1 recipient mice treated with and without CC4074 at 30 days after tumor cell injection. (n = 4 mice per group, **$p < 0.005$, by two-tailed Student's *t*-test).

mouse studies. HZ and HH performed ELISA. HZ, HH, GL, WH and AG monitored and analyzed phonotypes of mice. ML performed RNA-seq library preparation. JL and DS perform bioinformatics analysis on RNA-seq data. MM provided flow cytometry support. SZ, YZ, XZ, KYK and MAG provided intellectual input to the project. YH and YZ wrote the manuscript with all the other authors participating in discussion, data interpretation and manuscript editing. The authors declared there is no conflicts of interest.

Declaration of competing interest

The original work reported herein has not been published previously and is not under consideration for publication elsewhere. The authors declared there is no conflicts of interest.

Acknowledgements

We are grateful for Dr. Jianjun Shen and the MD Anderson Cancer Center next-generation sequencing core at Smithville (CPRIT RP120348 and RP170002), and the Epigenetic core in Institute of Biosciences and Technology at the Texas A&M University. This work was supported by grants from Cancer Prevention and Research Institute of Texas (RR140053 to YH, to RP170660 to YZ, RP180131 to DS), the John S. Dunn Foundation Collaborative Research Award (to YH and YZ), the National Institutes of Health grants (R01HL134780 and R01HL146852 to YH, R01GM112003 and R01CA232017 to YZ, R01AI136917 to KYK), the Welch Foundation (BE-1913 to YZ), the American Cancer Society (RSG-18-043-01-LIB to YH, RSG-16-215-01-TBE to YZ), and by an allocation from the Texas A&M University start-up funds (YH and DS).

Appendix A. Supplementary data

Supplementary data to this article can be found online at https://doi.org/10.1016/j.canlet.2019.09.013.

References

[1] F. Delhommeau, S. Dupont, V. Della Valle, C. James, S. Trannoy, A. Masse, et al., Mutation in TET2 in myeloid cancers, N. Engl. J. Med. 360 (22) (2009 May 28) 2289–2301.

[2] F. Lemonnier, L. Couronne, M. Parrens, J.P. Jais, M. Travert, L. Lamant, et al., Recurrent TET2 mutations in peripheral T-cell lymphomas correlate with TFH-like features and adverse clinical parameters, Blood 120 (7) (2012 Aug 16) 1466–1469.

[3] A. Tefferi, K.H. Lim, R. Levine, Mutation in TET2 in myeloid cancers, N. Engl. J. Med. 361 (11) (2009 Sep 10) 1117–1118 1117; author reply.

[4] L. Couronne, C. Bastard, O.A. Bernard, TET2 and DNMT3A mutations in human T-cell lymphoma, N. Engl. J. Med. 366 (1) (2012 Jan 5) 95–96.

[5] R. Itzykson, O. Kosmider, A. Renneville, V. Gelsi-Boyer, M. Meggendorfer, M. Morabito, et al., Prognostic score including gene mutations in chronic myelomonocytic leukemia, J. Clin. Oncol. 31 (19) (2013 Jul 1) 2428–2436.

[6] A. Tefferi, K.H. Lim, O. Abdel-Wahab, T.L. Lasho, J. Patel, M.M. Patnaik, et al., Detection of mutant TET2 in myeloid malignancies other than myeloproliferative neoplasms: CMML, MDS, MDS/MPN and AML, Leukemia 23 (7) (2009 Jul) 1343–1345.

[7] V. Grossmann, A. Kohlmann, C. Eder, C. Haferlach, W. Kern, N.C. Cross, et al., Molecular profiling of chronic myelomonocytic leukemia reveals diverse mutations in > 80% of patients with TET2 and EZH2 being of high prognostic relevance, Leukemia 25 (5) (2011 May) 877–879.

[8] C. Quivoron, L. Couronne, V. Della Valle, C.K. Lopez, I. Plo, O. Wagner-Ballon, et al., TET2 inactivation results in pleiotropic hematopoietic abnormalities in mouse and is a recurrent event during human lymphomagenesis, Cancer Cell 20 (1) (2011 Jul 12) 25–38.

[9] S. Chiba, Dysregulation of TET2 in hematologic malignancies, Int. J. Hematol. 105 (1) (2017 Jan) 17–22.

[10] L. Busque, J.P. Patel, M.E. Figueroa, A. Vasanthakumar, S. Provost, Z. Hamilou, et al., Recurrent somatic TET2 mutations in normal elderly individuals with clonal hematopoiesis, Nat. Genet. 44 (11) (2012 Nov) 1179–1181.

[11] K. Moran-Crusio, L. Reavie, A. Shih, O. Abdel-Wahab, D. Ndiaye-Lobry, C. Lobry, et al., Tet2 loss leads to increased hematopoietic stem cell self-renewal and myeloid transformation, Cancer Cell 20 (1) (2011 Jul 12) 11–24.

[12] M. Ko, H.S. Bandukwala, J. An, E.D. Lamperti, E.C. Thompson, R. Hastie, et al., Ten-Eleven-Translocation 2 (TET2) negatively regulates homeostasis and differentiation of hematopoietic stem cells in mice, Proc. Natl. Acad. Sci. U. S. A. 108 (35) (2011 Aug 30) 14566–14571.

[13] Z. Li, X. Cai, C. Cai, J. Wang, W. Zhang, B.E. Petersen, et al., Deletion of Tet2 in mice leads to dysregulated hematopoietic stem cells and subsequent development of myeloid malignancies, Blood 118 (17) (2011 Jul 29) 4509–4518.

[14] X. Zhang, J. Su, M. Jeong, M. Ko, Y. Huang, H.J. Park, et al., DNMT3A and TET2 compete and cooperate to repress lineage-specific transcription factors in hematopoietic stem cells, Nat. Genet. 48 (9) (2016 Sep) 1014–1023.

[15] S. Zang, J. Li, H. Yang, H. Zeng, W. Han, J. Zhang, et al., Mutations in 5-methylcytosine oxidase TET2 and RhoA cooperatively disrupt T cell homeostasis, J. Clin. Investig. 127 (8) (2017 Aug 01) 2998–3012.

[16] A.H. Shih, Y. Jiang, C. Meydan, K. Shank, S. Pandey, L. Barreyro, et al., Mutational cooperativity linked to combinatorial epigenetic gain of function in acute myeloid leukemia, Cancer Cell 27 (4) (2015 Apr 13) 502–515.

[17] T. Muto, G. Sashida, M. Oshima, G.R. Wendt, M. Mochizuki-Kashio, Y. Nagata, et al., Concurrent loss of Ezh2 and Tet2 cooperates in the pathogenesis of myelodysplastic disorders, J. Exp. Med. 210 (12) (2013 Nov 18) 2627–2639.

[18] J.R. Cortes, A. Ambesi-Impiombato, L. Couronne, S.A. Quinn, C.S. Kim, A.C. da Silva Almeida, et al., RHOA G17V induces T Follicular helper cell specification and promotes lymphomagenesis, Cancer Cell 33 (2) (2018 Feb 1) 259–273.

[19] M. Meisel, R. Hinterleitner, A. Pacis, L. Chen, Z.M. Earley, T. Mayassi, et al., Microbial signals drive pre-leukaemic myeloproliferation in a Tet2-deficient host, Nature 557 (7706) (2018 May) 580–584.

[20] Z. Cai, J.J. Kotzin, B. Ramdas, S. Chen, S. Nelanuthala, L.R. Palam, et al., Inhibition of inflammatory signaling in Tet2 mutant preleukemic cells mitigates stress-induced abnormalities and clonal hematopoiesis, Cell Stem Cell 23 (6) (2018 Dec 6) 833–849 e835.

[21] I. Ganan-Gomez, Y. Wei, D.T. Starczynowski, S. Colla, H. Yang, M. Cabrero-Calvo, et al., Deregulation of innate immune and inflammatory signaling in myelodysplastic syndromes, Leukemia 29 (7) (2015 Jul) 1458–1469.

[22] K.Y. King, M.A. Goodell, Inflammatory modulation of HSCs: viewing the HSC as a foundation for the immune response, Nat. Rev. Immunol. 11 (10) (2011 Sep 9) 685–692.

[23] E.M. Pietras, Inflammation: a key regulator of hematopoietic stem cell fate in health and disease, Blood 130 (15) (2017 Oct 12) 1693–1698.

[24] M. Dalamaga, E. Petridou, F.E. Cook, D. Trichopoulos, Risk factors for myelodysplastic syndromes: a case-control study in Greece, Cancer Causes Control 13 (7) (2002 Sep) 603–608.

[25] J.R. Cortes, T. Palomero, The curious origins of angioimmunoblastic T-cell lymphoma, Curr. Opin. Hematol. 23 (4) (2016 Jul) 434–443.

[26] W. Khayr, R.Y. Haddad, S.A. Noor, Infections in hematological malignancies, Dis. Mon. 58 (4) (2012 Apr) 239–249.

[27] K.S. Josefsdottir, M.T. Baldridge, C.S. Kadmon, K.Y. King, Antibiotics impair murine hematopoiesis by depleting the intestinal microbiota, Blood 129 (6) (2017 Feb 09) 729–739.

[28] H. Yan, M.T. Baldridge, K.Y. King, Hematopoiesis and the bacterial microbiome, Blood 132 (6) (2018 Aug 9) 559–564.

[29] F. Pan, T.S. Wingo, Z. Zhao, R. Gao, H. Makishima, G. Qu, et al., Tet2 loss leads to hypermutagenicity in haematopoietic stem/progenitor cells, Nat. Commun. 8 (2017 Apr 25) 15102.

[30] S.O. Abegunde, R. Buckstein, R.A. Wells, M.J. Rauh, An inflammatory environment containing TNFalpha favors Tet2-mutant clonal hematopoiesis, Exp. Hematol. 59 (2018 Mar) 60–65.

[31] A. Tsagaratou, E. Gonzalez-Avalos, S. Rautio, J.P. Scott-Browne, S. Togher, W.A. Pastor, et al., TET proteins regulate the lineage specification and TCR-mediated expansion of iNKT cells, Nat. Immunol. 18 (1) (2017 Jan) 45–53.

[32] M. Ko, J. An, H.S. Bandukwala, L. Chavez, T. Aijo, W.A. Pastor, et al., Modulation of TET2 expression and 5-methylcytosine oxidation by the CXXC domain protein IDAX, Nature 497 (7447) (2013 May 2) 122–126.